

Impacts of Reactor Configuration, Degradation Mechanisms, and Water Matrices on Perfluorocarboxylic Acid Treatment Efficiency by the UV/Bi₃O(OH)(PO₄)₂ Photocatalytic Process

Mojtaba Qanbarzadeh,[#] Dawei Wang,[#] Mohamed Ateia, Sushant P. Sahu, and Ezra L. Cates*Cite This: <https://dx.doi.org/10.1021/acsestengg.0c00086>

Read Online

ACCESS |



Metrics & More



Article Recommendations



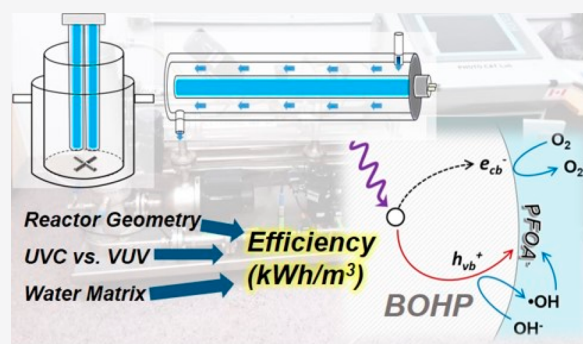
Supporting Information

ABSTRACT: Semiconductor photocatalysis is currently being explored as a treatment tool for wastewaters contaminated with poly-/perfluoroalkyl substances (PFAS), such as groundwater impacted by aqueous film-forming foams. While numerous catalysts have been shown to degrade perfluorocarboxylic acids (PFCAs) such as PFOA, research thus far has been confined to bench-scale evaluations that offer little insight into the practical aspects and potential energy efficiency expected during full-scale application. Herein, we advanced such understanding using the recently discovered Bi₃O(OH)(PO₄)₂ catalyst system (UV/BOHP) by first elucidating the basic PFCA degradation mechanisms and behavior, followed by comparisons among different photoreactor designs. The BOHP suspension degraded PFCAs primarily through direct heterogeneous oxidation by valence band holes, and kinetics correlated positively with chain length. Degradation of PFCAs was further compared between stirred immersion photoreactors, bench-scale confined-flow high-intensity slurry photocatalytic reactors (CHISPRs), and a larger commercial CHISPR system. Complete degradation (>99%) of long-chain PFCAs was observed in the immersion reactors within 60 min, while the CHISPRs degraded all PFAS tested within 20 min; however, control tests revealed that direct photolysis by vacuum UV was the main driver in the CHISPRs. Despite their faster kinetics, the energy consumption (per order removal) of PFOA photolysis in the unmodified CHISPRs was significantly higher (51–124 kWh/m³) compared to PFOA photocatalysis in the immersion reactors (25 ± 4 kWh/m³). Based on these findings, practical photoreactor design criteria were proposed which incorporate both photolysis and photocatalysis, and which have implications beyond just the UV/BOHP process.

KEYWORDS: PFAS, Photocatalysis, Bismuth phosphate, Photoreactor, Vacuum UV

INTRODUCTION

In the wake of intensifying research on poly-/perfluoroalkyl substance (PFAS) contamination, the need for practical removal methods within nearly every sector of water treatment and remediation is now evident, including drinking water, wastewater, groundwater, leachate, and industrial discharge.^{1–4} Current technological trends suggest that adsorbents and ion exchange resins can contribute to PFAS control in municipal water and wastewater treatment scenarios handling MGD-range flows (10³–10⁴ m³/d) and relatively low PFAS loading.^{5,6} Destructive processes that produce no hazardous residuals, on the other hand, may prove more cost-effective for smaller decentralized operations associated with contaminated groundwater sites, landfills, and industrial effluents, as examples. While conventional homogeneous advanced oxidation processes based solely on •OH generation are ineffective in destroying PFAS,⁷ photocatalytic treatment is a promising route. Several unconventional wide band gap semiconductor photocatalysts have been shown to degrade perfluorocarboxylic



acids (PFCAs) under UV irradiation, including β -Ga₂O₃, In₂O₃, InOOH, and BN.^{8–11}

Recently, we demonstrated photocatalytic degradation of perfluorooctanoic acid (PFOA) by bismuth phosphate semiconductors, including BiPO₄ submicrometer particles (*n* monoclinic) and Petitjeanite Bi₃O(OH)(PO₄)₂ microparticles (BOHP).¹² In benchtop UVC immersion reactors, a suspension of BOHP was shown to outperform BiPO₄ and β -Ga₂O₃, achieving complete degradation of PFOA in under 60 min and >60% fluoride liberation in 120 min.¹² Results showed that acidic conditions (pH < 4.5) were indispensable to rapid PFOA degradation by BOHP, as they promoted

Received: July 20, 2020

Revised: October 2, 2020

Accepted: November 4, 2020



positive charge on the catalyst surface which attracted the deprotonated PFOA carboxylate headgroup. Overall, BOHP may be well-suited for practical application in UV photoreactors due to its chemical stability, low toxicity, high catalytic activity, and physical durability.^{12,13} With an estimated band gap of 3.90 eV,¹² photoexcitation is achievable using UVB LEDs (e.g., 290 nm) or more conventional mercury lamps.

Photocatalytic water treatment techniques are notoriously difficult to scale-up and transfer out of the laboratory; therefore, we assert that further development of the UV/BOHP process should address reactor design aspects early on, rather than focusing solely on degradation mechanisms and catalytic behavior at this time. Moreover, any interpretation of bench-scale photocatalytic performance data should consider what type of full-scale reactor might be used for real-world application of the process.

Most laboratory studies on photocatalytic water treatment techniques have employed immersion photoreactors, wherein a mercury lamp assembly is immersed into a magnetically stirred cylindrical vessel containing suspended catalyst particles, in an annular configuration. Lamp-to-wall distances (annulus width) are typically a few centimeters but vary widely among studies. Their impact on treatment efficiency is also overlooked. While simple to construct for lab tests, this reactor type is not typically used for larger-scale systems, wherein flow-through designs using mainly static mixing are common to pilot-scale experimental systems.^{14–17} Thus, the only widely applied commercial photocatalytic system is the Purifics Photo-cat®, which uses a TiO₂ slurry in designs with treatment capacities ranging up to 4 MGD (4264 m³/d).¹⁸ This system—to which we refer generically herein as a confined-flow, high-intensity, slurry photocatalytic reactor (CHISPR)—employs a design that differs drastically from typical laboratory reactors. (For a detailed description of the Photo-cat® system, the reader is referred to ref 19.) The distinguishing features of CHISPRs are flow-through configuration with a narrow annulus width; high flow velocity (and thus turbulence); and high ratio of lamp power to reactor volume ($P:V$ ratio). For the Photocat-L system, these values are 3 mm, 1.8 m/s, and 349 W/L, respectively. Scale-up to MGD-range treatment rates has been achieved by arranging numerous CHISPRs in series, with full-scale commercial units employing up to 360 kW of low pressure mercury lamp wattage.¹⁸ Because of the different configurations, photocatalytic behaviors observed for any catalyst/contaminant combination have the potential to differ significantly between immersion reactors and CHISPRs.

Our preliminary experimentation with the UV/BOHP process also revealed that the degradation behavior of PFAS in photocatalytic reactors may be affected significantly by the type of low-pressure mercury lamp employed, i.e., VUV-emitting (254/185 nm; “ozone generating”) or non-VUV emitting (254 nm UVC emission only; “ozone-free”). The two types differ only in the purity and thus VUV transmittance of the quartz glass components of the bulb and protective sleeve. Direct photolysis of PFAS has been observed by other researchers for both UVC and VUV, though the former is much less efficient and typically neglected in immersion reactor studies.^{20,21} Given the dose rates used in CHISPRs, however, the effects of both types of photolysis should be carefully considered in addition to photocatalytic degradation.

The broader goal of this work is to advance understanding of the UV/BOHP process as it applies to practical treatment of PFAS-contaminated groundwaters. The scope of our objectives

included (1) to elucidate the photocatalytic mechanisms and behavior of BOHP which may be affected by operational conditions; (2) to assess the ability of BOHP to degrade a wider range of PFAS species; (3) to determine the impacts of realistic water matrices on degradation kinetics; and (4) to compare performance and energy efficiency between different reactor configurations. Experiments were conducted using benchtop immersion reactors and custom-made bench-scale CHISPRs, as well as a pilot-scale Purifics Photo-cat® system (Figure 1).

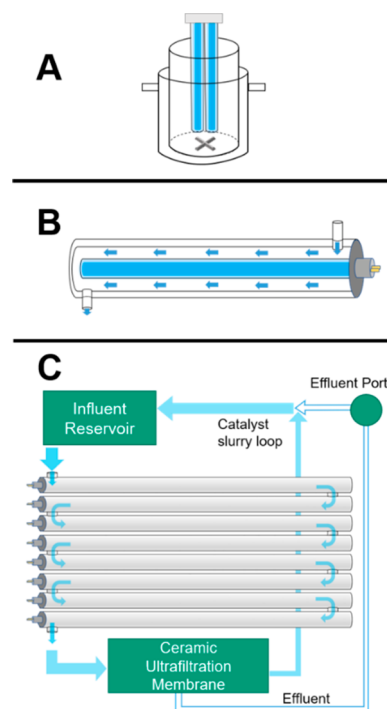


Figure 1. Photoreactor configurations used in this study (mercury lamps depicted in blue), including (A) immersion photoreactor, (B) benchtop CHISPR, and (C) commercial CHISPR system with catalyst separation and effluent recycle (lamps are mounted within the tubes similar to in part B). All reactors were equipped with outer cooling jackets through which tap water flowed. Photographs are shown in Figure S1.

EXPERIMENTAL METHODS

Materials. Stock chemical sources and purities are provided in the Supporting Information (Text S1). BOHP micro-particles were prepared using hydrothermal syntheses, as described in our previous work.¹² Diluted HCl and NaOH (~0.1 M) were used to adjust the pH of the precursor solutions. Distilled–deionized water (DDI) of resistivity 18 MΩ·cm or tap water were used in all experiments.

Analyses. Chemical analyses of PFAS and other analytes, as well as catalyst material characterization methods, are provided in the Supporting Information (Text S2).

Photoreactors and Photocatalysis Experiments. Photocatalytic tests were performed in three photoreactor systems, depicted in Figures 1 and S1, and the parameters are listed in Table 1. The Photo-cat® system was operated with a total system volume of 16 L, typically using a tap water matrix, with a recycle flow rate of 25 L/min. Tap water parameters are listed in Table S1. The amount of BOHP added was 20 g (1.25

Table 1. Characteristics of Photoreactor Systems Used in This Study

	immersion photoreactors	bench-scale CHISPR	pilot-scale CHISPR system
individual lamp wattage (W)	7.2 ^a	48 or 57	75
number of lamps	1	1	8
operation mode	batch	recirculation	recirculation
wavelengths (nm)	254	254 or 185/254	185/254
catalyst conc. (g/L)	1.8	1.8	1.25
typical water matrix	acidified DDI water	acidified DDI water	tap water

^a18 W lamp submerged partway (0.4)

g/L), as pre-experiments revealed that greater amounts did not result in faster PFOA degradation, and the synthesis requirements were prohibitive. The unit was also equipped with a rack cooling system comprising steel jackets around each photoreactor through which tap water was pumped to keep the treatment water cool during operation in recycle mode. The typical steady state temperature of the Photo-cat® water was 38 °C. Additional details of the Photo-cat® system can be found in Gerrity et al.¹⁹ Smaller, bench-scale CHISPRs were also constructed to emulate the annulus width and slurry flow velocity of the reactors in the commercial system while providing a simplified treatment loop for greater control over photocatalysis/photolysis conditions. These reactors were equipped with either 254 nm emission lamps or 185/254 nm lamps. Full details of the reactors are included in Text S3.

Immersion Photoreactor Experiments. Experiments in the bench immersion photoreactors were performed as reported previously, though some experiments used a 185/254 nm lamp of equivalent submerged wattage.¹² For scavenger experiments, an initial PFOA concentration of 0.13 mM was used, and sodium oxalate, isopropanol (IPA), and superoxide dismutase (SOD) were added at 2.5 mM, 14.5 mM, and 6.0 U/mL, respectively. In the experiments using O₂ and N₂ bubbling, the solutions were bubbled continuously with the gas for 2 h before starting the irradiation, as well as during the experiments. For evaluation of potential quenching by

groundwater matrix components, Suwannee River NOM, NaCl, and Na₂SO₄ were used as sources of NOM, Cl⁻, and SO₄²⁻, respectively (Text S1). Samples collected for high-performance liquid chromatography (HPLC) and ion chromatography (IC) analyses were filtered using 0.2 μm poly(ether sulfone) (PES) filters.

Commercial Pilot-Scale CHISPR Experiments. Tap water spiked with PFAS was prepared externally and then transferred into the Photo-cat® unit via the influent reservoir. Before turning on the UV lamps, the unit was run in the dark mode for 2 h to achieve adsorption/desorption equilibrium and homogeneously disperse the contaminant(s) throughout the system. In a typical photocatalytic experiment for high initial concentrations (0.13 mM), irradiation was conducted for 3 h with the water-cooling system on. Samples of 50 mL were taken for analysis every 1 h from the effluent sampling port; this port is located after the membrane unit, and the effluent is thus free of catalyst particles. Before each experiment, the CHISPR was flushed for 10 min with tap water to remove the residual PFAS from the system. To prepare the unit for experiments using low initial PFAS concentrations (ppb-range), the unit was flushed with tap water for 6 h to achieve a measured residual PFOA concentration of <0.4 ppb, as determined by LC-MS/MS analysis.

Bench-Scale CHISPR Experiments. The BOHP/PFAS slurries were prepared externally by mixing in DDI water. In a typical experiment, the slurry was first transferred into the system via the polypropylene graduated cylinder, which served as an influent reservoir (Figure S1). Before turning on the lamp, the slurry was circulated through the system in the dark mode for 15 min to achieve adsorption/desorption equilibrium of the system, while the outer cooling jackets were continually flushed with tap water to maintain constant temperature. During treatment, sample aliquots were collected via a valve, with the first 5 mL returned to the influent reservoir to minimize the interference from the residual solutions in the valve. Then, 3 mL was collected. Samples were filtered using 0.2 μm PES filters. After each experiment, a cleaning procedure was performed to remove the residual PFAS from the bench-scale CHISPR system. Tap water was first pumped through the whole system for at least 30 min. Then, 400 mL of DDI water

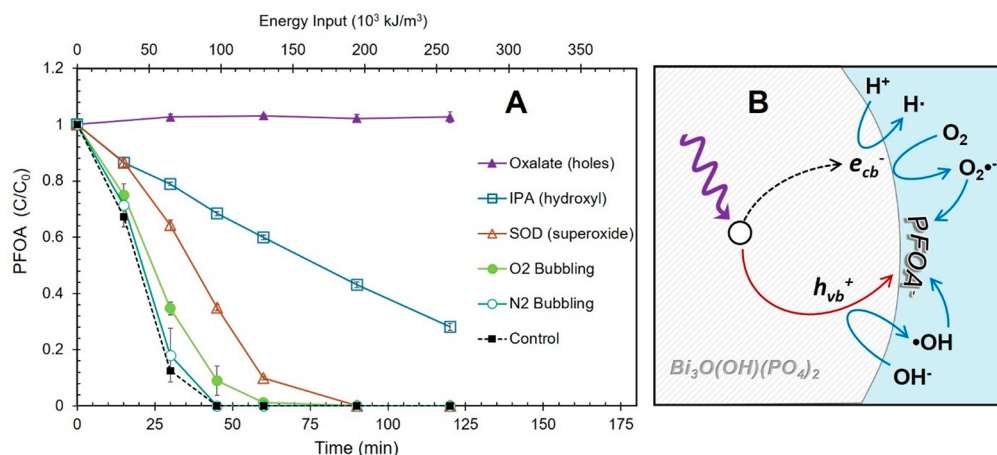


Figure 2. Photocatalytic degradation mechanisms of PFOA by UV/BOHP. (A) Results of immersion reactor scavenger studies using UVC irradiation (254 nm) with scavengers and target active species indicated in parentheses. Error bars represent standard deviations of experiments performed in triplicate. (B) Hypothesized mechanisms of PFOA degradation. Red arrows show primary mechanisms while blue arrows show secondary mechanisms.

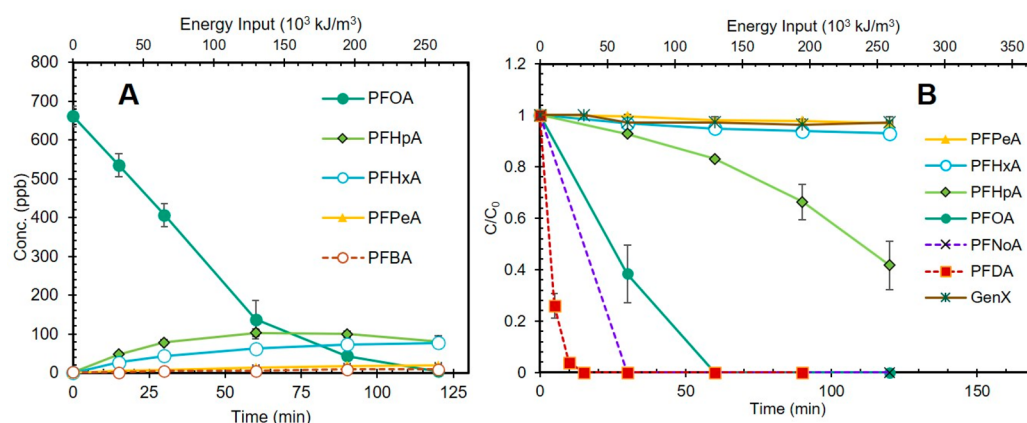


Figure 3. (A) Concentrations of PFCAs during PFOA degradation by UV/BOHP using an immersion reactor and 254 nm irradiation ($C_0 = 660$ ppb). (B) Degradation kinetics of various PFCAs and GenX spiked individually in the immersion reactor ($C_0 = 53$ ppm). Experiments were performed using DDI matrix adjusted to initial pH of 4. Error bars represent standard deviations of experiments performed in triplicate.

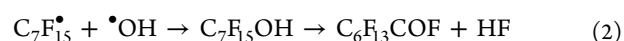
was circulated through the reactor for 10 min and then discharged. This procedure was repeated three times before starting new experiments.

RESULTS AND DISCUSSION

Characterization. Data pertaining to particle morphology, phase purity, and zeta potential of BOHP were included in our previous work.¹² Herein we additionally determined the pH of zero charge (PZC) of BOHP to be approximately 5.9 (Figure S2), which is consistent with our previous result of positive zeta potential at pH 4 and negative potential at neutral pH.¹²

Photocatalysis Mechanism. Classical photocatalytic water treatment employs semiconductors such as TiO_2 to produce surface-bound and bulk phase reactive oxygen species—namely $\cdot\text{OH}$ and $\text{O}_2^{\cdot-}$ —which in turn oxidize target contaminants. Our previous work, as well as other reports of photocatalytic PFOA degradation,^{10,12,22} found that catalyst surface properties favoring PFOA adsorption strongly enhanced degradation and mineralization kinetics. The direct heterogeneous reaction between PFAS and valence band holes (h_{vb}^+) was thus speculated to be the primary mode of action by UV/BOHP. To confirm the role of h_{vb}^+ herein, individual active species were quenched with appropriate scavengers during UV/BOHP treatment to reveal those which contributed most to PFOA degradation. Addition of oxalate as a h_{vb}^+ scavenger^{23,24} completely halted degradation as seen in Figure 2A; this confirms that h_{vb}^+ plays a vital role but does not indicate whether it is through direct heterogeneous reaction or an indirect mechanism involving radical formation. Isopropanol and SOD were added to quench $\cdot\text{OH}$ and $\text{O}_2^{\cdot-}$,^{9,23} respectively, and the results are also shown in Figure 2A. Quenching of $\cdot\text{OH}$ by IPA markedly slowed PFOA degradation, with methanol and *t*-butanol having a similar effect (data not shown). While direct reaction of PFOA with $\cdot\text{OH}$ is known to be inefficient in homogeneous advanced oxidation,⁷ several works involving the reaction of PFOA at liquid–solid interfaces have reported similar results, including in photocatalytic and electrochemical systems.^{9,25–27} Relating to the same behavior observed during PFOA degradation by a In_2O_3 photocatalyst, Wu et al. proposed that $\cdot\text{OH}$ reacts with perfluoroalkyl radical intermediates formed by reaction of PFOA with h_{vb}^+ (Reaction 2) and thus accelerates the stepwise chain-shortening mineralization process.⁹ Aside from aiding in mineralization, the manner in which $\cdot\text{OH}$ contributes to

parent compound degradation is not clear at this time, though an apparent synergism upon exposure of adsorbed PFOA to $\cdot\text{OH}$ and h_{vb}^+ simultaneously has been noted by others.^{9,11} Finally, quenching of $\text{O}_2^{\cdot-}$ resulted in a measurable impairment of PFOA degradation, suggesting possible minor contribution of $\text{O}_2^{\cdot-}$ in degrading PFOA. Activity of $\text{O}_2^{\cdot-}$ in degrading PFOA has been reported by others.²⁸ The hypothesized primary mechanism of PFOA oxidation is shown below, in agreement with other photocatalysis studies:⁹



The effect of both excess and diminished dissolved O_2 was studied by purging the suspensions with O_2 and N_2 gases, respectively, during irradiation (Figure 2A). Additional O_2 was expected to enhance PFOA degradation by increasing $\text{O}_2^{\cdot-}$ generation, but interestingly, bubbling with neither gas resulted in enhancement compared to the air atmosphere control. In the case of the O_2 -bubbled experiment, the BOHP particles became less stable in suspension and were observed forming particle–bubble aggregates that resulted in some loss from the reactor. We hypothesize that O_2 ionosorption and/or attack by $\text{O}_2^{\cdot-}$ resulted in neutralization of positively charged BOHP surface groups, such as oxygen vacancies; this charge neutralization in turn led to flocculation that impeded photocatalysis by inhibiting mass transfer to the available surface area and caused catalyst self-shading. While this explanation is not proven, the results clearly indicate that UV/BOHP is not enhanced by the addition of O_2 . Moreover, the lack of any quenching effect by N_2 bubbling (and thus removal O_2) suggests that H^+ might serve as a BOHP conduction band electron acceptor, and the presence of O_2 is not a prerequisite for PFOA degradation under acidic conditions. The proposed photocatalytic mechanism is depicted in Figure 2B.

The kinetics of PFOA degradation by UV/BOHP with a ppb-range starting concentration are shown in Figure 3A, along with the concentration profiles of shorter-chain PFCA intermediate products. PFOA was completely degraded (>99%) after 120 min, which was slower compared to the ppm-range starting concentration and consistent with an

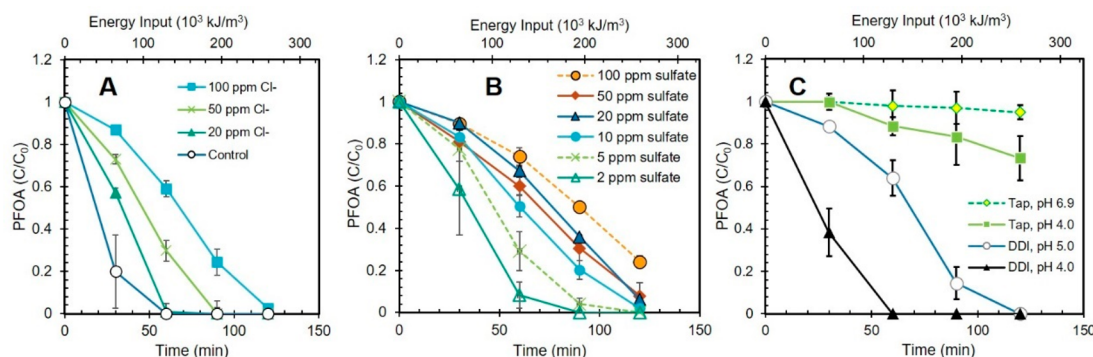


Figure 4. Effects of water matrix contents on PFOA degradation by UV/BOHP in the immersion photoreactor (254 nm). (A) Effect of copresent Cl^- and (B) sulfate anions on PFOA degradation kinetics. (C) Comparison of tap water and DDI matrices at different pH values. Error bars show standard deviations of triplicate experiments; $C_{0,PFOA} = 0.13$ mM.

adsorption-dependent mechanism; therein, a lower solution phase PFOA concentration resulted in a lower adsorbed-phase concentration at equilibrium, thereby decreasing the probability of interaction with photogenerated charge carriers. All short-chain PFCAs included in our analyses were detected and increased in concentration as PFOA was degraded, with the exception of perfluoroheptanoic acid (PFHpA) which began to decline after 90 min. The data suggest that PFCAs of six carbons or less are not degraded by BOHP under these conditions, which is further confirmed by the data in Figure 3B. Therein, PFCAs (C4–C10) and 2,3,3,3-tetrafluoro-2-(heptafluoropropoxy)propanoic acid (GenX) were spiked individually at a high concentration (0.13 mM) into separate solutions for treatment by UV/BOHP. A distinct dependence of degradation rate on PFCA chain length was observed, with perfluorodecanoic acid (PFDA) showing the fastest degradation and C4–C6 compounds showing negligible degradation. This trend can be explained by adsorption behavior, which is also known to be generally dependent on PFCA chain length.²⁹ The short-chain compounds known for poor adsorption had limited interaction with the catalyst surface and direct reaction with $h_{\nu b}^+$ was inefficient. Additionally, no degradation of GenX was observed, despite having a similar chain length to that of PFHpA. The result was attributed to the methyl group on the α carbon, which is known to cause a steric hindrance that interferes with both adsorption and reactions that target the carboxylate headgroup.^{30,31}

Effects of the Water Matrix. Applicability of the UV/BOHP process to real waters was first assessed by singly introducing potential quenching species at concentrations typical to groundwaters, including natural organic matter (NOM), Cl^- , and SO_4^{2-} . As seen in Figure S3a, the presence of Suwanee River NOM had no significant effect on PFOA degradation at any of the test concentrations, which ranged up to 7.3 mg/L dissolved organic carbon (DOC). Yet, we found that BOHP could readily degrade NOM, as evidenced by up to ~80% reduction in DOC after 2 h, with accompanying improvements in UV transmittance (Figure S3b,c). The finding of NOM degradation, but a lack of interference in PFOA degradation, indicates a contrasting photocatalytic mechanism. Anionic PFOA was readily attracted to the positively charged catalyst surface where it directly reacted with $h_{\nu b}^+$. Humic substances, on the other hand, have $pK_a > 4$,³² were thus mainly protonated and neutral at $pH < 4$, and would be sterically hindered from direct reaction with the catalyst surface. It is therefore likely that NOM was degraded

primarily by reactive oxygen species that diffused from BOHP to the bulk solution.

Since groundwater often contains elevated Cl^- and SO_4^{2-} concentrations, the impacts of these anions on UV/BOHP were evaluated at environmentally relevant concentrations. The effects of concentrations up to 100 ppm on PFOA degradation kinetics are shown in Figure 4 a,b, respectively. The presence of both anions negatively impacted PFOA degradation rate, with SO_4^{2-} having a greater impact on a per molar basis. Literature reports of effects of Cl^- on semiconductor photocatalytic water treatment are inconsistent (and largely exclusive to TiO_2), with some studies reporting significant quenching,^{33–35} some reporting enhancement effects,³⁶ and others reporting a negligible effect.^{37,38} In the case of quenching, the mechanisms were also inconsistent and speculative, including both adsorption/surface effects and $h_{\nu b}^+$ scavenging. Iguchi et al. conclusively showed that Cl^- was oxidized by the $h_{\nu b}^+$ of layered double hydroxide photocatalysts to produce HOCl.³⁹ Given the wide band gap and oxidizing ability of BOHP, we speculate this is also the case here. Sulfate, on the other hand, would not be oxidized further but likely acted by adsorbing to the BOHP surface as reported for other materials; this in turn neutralized positive surface charge and created a potential barrier that interfered with the PFOA– $h_{\nu b}^+$ direct reaction.^{37,40} As seen in the data, the quenching effect begins to plateau at SO_4^{2-} concentrations greater than 10 ppm. Additional increases in the SO_4^{2-} concentration resulted in diminishing increases in quenching, consistent with the catalyst surface approaching a saturated adsorption capacity.

Due the detrimental effects of anions (Cl^- , SO_4^{2-} , and possibly others), there likely exists a trade-off with respect to intentional acidification of the UV/BOHP process. Lower pH improves surface charge and contaminant-catalyst contact, but the counterion component of any acid may induce quenching effects—particularly for alkalinity-bearing waters that require more copious acid addition to reach pH 4. To elucidate, additional PFOA kinetics comparisons were performed in the immersion reactor using tap water and DDI matrices, with various adjustments made to initial pH values with PFOA degradation kinetics shown in Figure 4C. (Water quality parameters of the employed tap water are shown in Table S1, including Cl^- and SO_4^{2-} concentrations of 7.7 and 10.8 ppm, respectively, and alkalinity of 12.8 mg/L- $CaCO_3$.) In DDI water, PFOA degradation rate was highly sensitive to pH, as we found previously.¹² For the pH 5 water, distinct accelerating degradation kinetics were observed as HF was generated in the

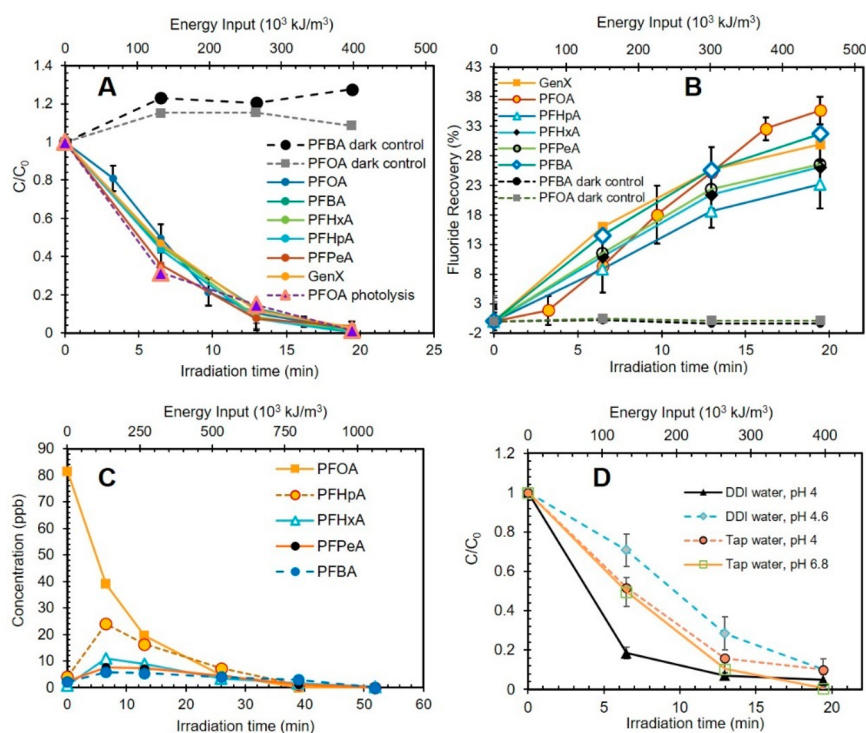


Figure 5. Results of commercial CHISPR (Photocat) experiments (185/254 nm). (A) Degradation of PFCAs spiked individually in the Photocat® system loaded with BOHP in tap water matrix and (B) associated fluoride liberation ($C_{0,\text{PFCA}} = 0.13 \text{ mM}$, $\text{pH}_0 \approx 6.8$). (C) Degradation of PFOA and intermediate products at low concentration ($C_{0,\text{PFOA}} = 81 \text{ ppb}$) in tap water. (D) PFOA degradation comparison between different water matrices. For CHISPR kinetic data, the degradation ratios are plotted versus “irradiation time”, which includes only the portion of the residence time spent within the actual photoreactor components of the system (Table S2). All experiments used an initial pH of approximately 6.8 unless otherwise indicated.

unbuffered solution and caused a drop in the pH. For tap water experiments, PFOA degradation was heavily suppressed both for natural pH conditions (6.9) and when acidification to pH 4 was employed. Considering the background Cl^- and SO_4^{2-} content of the tap water, as well as the substantial additional HCl added to remove alkalinity and lower the pH, photocatalysis was undoubtedly quenched by anions during this experiment. Overall, these results suggest that alkalinity is problematic for UV/BOHP photocatalysis, though the use of other acids for lowering the pH may be less detrimental than HCl.

Commercial CHISPR Reactor Results. Figure 5A,B shows the degradation and F^- recovery, respectively, of singly spiked PFCAs and GenX in tap water by the commercial CHISPR loaded with BOHP. While the observed degradation kinetics were faster than those in the immersion reactor when plotted vs irradiation time, the energy per unit volume values plotted on the secondary X-axes show that the commercial reactor used 2.5 times more lamp energy to achieve the same degree of removal. Energy efficiency aspects are discussed in further detail in a later section. Degradation of all PFAS proceeded at similar rates in this reactor, as did the PFOA control experiment using no BOHP, which together indicates that photolysis was responsible and not photocatalysis. Unlike the lamps used in the immersion reactor experiments discussed above, those in the commercial reactor included 185 nm VUV emissions capable of directly photolyzing most PFAS.^{20,41} Overall, F^- recovery was significantly lower than that observed previously in the immersion reactor for PFOA,²⁵ with PFHpA showing the lowest ($23 \pm 4\%$) and PFOA the highest ($36 \pm$

2%), though no clear trend was observed. Since significant turbulence occurred where the recycled effluent and slurry reenter the influent reservoir (Figure 1C), air stripping is suspected to have resulted in loss of HF and other intermediate fluorinated compounds from the system. The data in Figure 5C show the appearance of sequentially shorter-chain PFCAs upon degradation of PFOA in the CHISPR, though other intermediates cannot be ruled out. With an initial PFOA concentration of 81 ppb in that experiment, all PFCA compounds were reduced to below detection limits (Table S3) within 50 min, with the exception of PFHxA ($C_{\text{final}} = 190 \text{ ppt}$).

Tap water was used in most commercial CHISPR experiments due to the extensive flushing requirements of the unit, though a limited number of experiments were completed with DDI matrix for comparison. As seen in Figure 5D, PFOA degradation was fastest in acidified DDI, suggesting that BOHP photocatalysis contributed to degradation to some extent in the reactor under these conditions. Furthermore, the aforementioned trade-off between acidification and anion addition in the case of alkalinity-bearing water was confirmed; since the tap water required more HCl to reach pH 4, the additional quenching from Cl^- counteracted any benefit to the BOHP surface charge, and degradation in tap water was largely photolysis-driven and insensitive to pH. Lastly, the faster degradation in tap water, compared to DDI at pH 4.6, may have been due to the presence of sulfate in the former. While we found sulfate to impair photocatalysis, it has been reported to undergo photolysis under VUV irradiation to form $\cdot\text{OH}$ ⁴²

and, thus, might provide enhancement when photolysis is the dominant mechanism.

Contributions of Photocatalysis and Photolysis. The results of commercial CHISPR experiments overall exhibited a starkly different behavior than those using the bench immersion reactors, with important implications in transferring the UV/BOHP process from the lab to the field. Comparison of the two is complicated by the existence of VUV emissions in CHISPR and apparent weak contribution of UVC photocatalysis relative to VUV photolysis. To explicitly separate these phenomena, tests were performed in bench-scale CHISPRs with irradiation and flow conditions similar to the reactors in the Photo-cat® system, and with option to be fitted with either of two lamp types—185/254 or 254 nm-only. Figure 6 shows comparisons of PFOA degradation using both

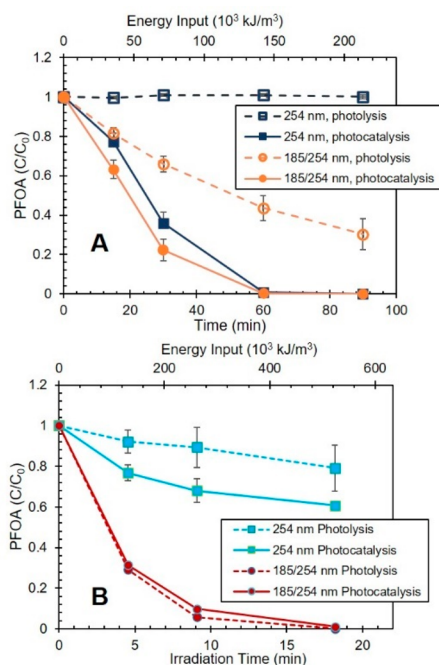


Figure 6. Effect of lamp type on PFOA photocatalysis (with BOHP) and photolysis (no catalyst) in both the (A) immersion reactor and (B) bench-scale CHISPR. $C_{0,PFOA} = 0.13$ mM in DDI water adjusted to pH with HCl.

immersion and CHISPR reactors fitted with the various lamp types. For the immersion reactor, photolysis of PFOA in the absence of any catalyst was observed for 185/254 nm irradiation, but not for 254 nm-only irradiation (Figure 6A). With BOHP present, the addition of the VUV emissions had surprisingly little effect on the kinetics. This result shows that PFOA degradation in the immersion reactor was dominated by photocatalysis even with VUV present. In the CHISPR, some PFOA photolysis by 254 nm-only irradiation was observed, owing to the higher average intensity in this reactor. The rate of degradation by 254 nm increased only slightly with BOHP added (Figure 6B), indicating a weaker photocatalytic effect compared to the immersion reactor. Under 185/254 nm irradiation, PFOA degradation rate was the same in the CHISPR whether BOHP was present or not, confirming that photolysis was dominant in this reactor type. We note that this behavior is only applicable to degradation of PFOA and likely longer-chain PFCAs as well. Tests performed using PFBA as the target contaminant revealed degradation by VUV

photolysis in both reactor types, but no contribution from BOHP photocatalysis in either case (data not shown). In fact, the presence of BOHP in the immersion reactor detracted slightly from PFBA degradation by attenuating VUV photons.

Reactor Design Evaluation. As seen above, even with the same photocatalyst, water matrix, target contaminant, and irradiation wavelengths, the immersion and CHISPR reactors demonstrated starkly different treatment behaviors. We hypothesized this contrast to have resulted from two aspects of their respective designs. First, VUV radiation is attenuated by water, and thus its effects radiate less than a centimeter from the source. With an annulus width of 3 mm, the CHISPR reactor contained all of the flow within range of the VUV to result in a greater contribution of photolysis. In the immersion reactor, however, only a small fraction of the volume was irradiated by VUV at any given time, thus limiting its overall contribution to PFOA degradation. Second, the 254 nm (UVC) component of mercury lamp emissions is ~ 10 times more intense than the VUV and has greater penetration depth into solutions.⁴³ With the CHISPR reactor, we suspect that a significant fraction of the UVC emissions was absorbed by the reactor walls (i.e., wall losses). Catalyst particles within the annulus would also experience a very high UVC intensity, potentially generating charge carriers faster than PFOA could transfer to their surfaces, causing a greater portion of h_{ν}^+ to be wasted (i.e., saturation losses). In contrast, with the greater lamp-to-wall distance and lower $P:V$ ratio of the immersion reactor, that system likely experienced much lower degrees of both types of losses, thus permitting more of the UVC energy to drive photocatalytic reactions. To demonstrate this theory, two additional bench-scale CHISPRs were constructed with double and quadruple the original annulus width (6 and 12 mm, respectively), while keeping the lamp power fixed. Results of PFOA degradation tests in all three CHISPRs, equipped with 185/254 nm lamps, are shown in Figure 7. Therein, it was found that as annulus width increased, the contribution of UVC photocatalysis relative to VUV photolysis increased.

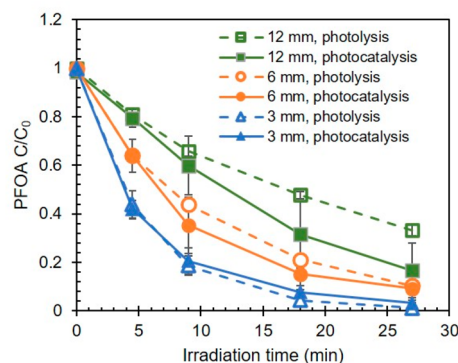


Figure 7. Comparison of photocatalytic (BOHP present, solid lines) and photolytic (no catalyst, dashed lines) PFOA degradation in CHISPR reactors with various annulus widths ($C_0 = 0.13$ mM in DDI, pH₀ 4).

Treatment Efficiency Comparison. In comparing different reactor systems for PFAS degradation, data concerning only kinetics can be misleading, as it does not inform on the treatment energy efficiency (e.g., kJ/m³) and treatment rate potential (e.g., m³/h, meeting the target effluent concentration) of a system. Processes offering fast degradation

kinetics can be accommodated in reactors with shorter residence times and smaller volumes, which, for photocatalysis, implies the additional benefit of requiring less catalyst material. Nonetheless, the energy requirements for destructive treatment of PFAS-contaminated waters remain the most challenging limitation, and therefore, a process with slower kinetics that requires longer residence time and larger footprint may in fact be preferred if it is overall more energy efficient.

For photoreactors using the same type of UV source, the electrical energy per log order reduction (EE/O) method offers a valid means of quantitatively comparing treatment efficiencies of different reactor systems.⁴⁴ The EE/O (kWh/m³, per order) for batch or recirculating reactors is calculated as follows:

$$EE/O = \frac{P}{-\log(C/C_0) \left(\frac{V}{t}\right) (3600)}$$

where P is the total electrical power of UV lamp(s) in the reactor (kW), C/C_0 is the contaminant removal ratio, V is the total volume of the treated water (m³), and t is the reaction time (s). This equation does not include other forms of energy consumption, such as pumping, since radiation sources account for the majority of electricity use in UV-based advanced redox processes. Calculated EE/O values for select experiments herein are shown in Table 2. Overall, the

Table 2. Comparison of EE/O Values Obtained from PFOA Degradation in the Reactors Used in This Study^a

reactor type	PFOA, with BOHP, EE/O (kWh/m ³)	PFBA, no catalyst, EE/O (kWh/m ³)
immersion reactor	25 (±4)	92 (±1)
commercial CHISPR, 3 mm	51 (±5)	85 (±6)
bench-scale CHISPR, 3 mm	124 (±22)	153 (±52)
bench-scale CHISPR, 6 mm	84 (±19)	127 (±3)
bench-scale CHISPR, 12 mm	70 (±39)	111 (±2)

^aIn all cases, 185/254 nm lamps and DDI water matrix at pH₀ = 4 were used, with the exception of the PFBA without catalyst in the commercial CHISPR, for which only tap water data at natural pH was obtained. Mid-range time values and their associated C/C_0 values from the kinetic curves were used for EE/O calculation. Standard deviations (±SD) are indicated.

immersion reactor system degraded PFOA via BOHP photocatalysis/VUV photolysis more energy-efficiently than the CHISPRs due to the greater lamp-to-wall distance, lower $P:V$, and efficient use of UVC photons as discussed previously. This reactor was also roughly as efficient or more efficient in photolyzing PFBA, compared to the CHISPRs. From a photolysis perspective, a greater lamp-to-wall distance results in slower kinetics by increasing the portion of the volume receiving negligible VUV photons; however, at the same time, elimination of wall losses results in more PFAS degradation per lamp wattage employed, and thus efficiency improves. This effect was observed more explicitly in the comparison of bench-scale CHISPRs with varying annulus width. For both PFOA photocatalysis/photolysis and PFBA photolysis, EE/O decreased as the lamp-to-wall distance increased.

The immersion reactor and CHISPR configurations also differ in how the water is mixed during treatment, with the

former using magnetic stirring and the latter relying on static mixing from flow through the reactor. For systems using low $P:V$, mixing is vitally important in cycling water from low intensity zones closer to the lamp(s) and for minimizing the mass transfer limitations of heterogeneous photocatalysis. From a design perspective, the statically mixed nature of the CHISPR concept is limiting, as turbulence cannot be controlled independently of flow rate. We therefore postulate that the most efficient design for degradation of long-chain PFCAs by UV/BOHP can be achieved in an immersion type reactor equipped with axial impellers, as has been proposed by others.⁴⁵ This configuration would be conducive to both efficient photon utilization and mixing and better able to take advantage of both VUV and UVC emissions. Moreover, individual modules could be arranged in-series and parallel to achieve a desired treatment rate and will be the subject of future work. Degradation of short-chain PFCAs and GenX are treated more efficiently by VUV photolysis without BOHP; therefore, a sequential-type treatment scheme using photocatalysis-optimized reactors followed by photolysis-optimized reactors may offer the most efficient route to comprehensive PFAS removal.

Compared to existing technologies, the observed EE/O values for UV/BOHP demonstrate that the process is competitive at this stage of development, at least for treatment of waters containing less than ~10 ppm of Cl⁻ and/or SO₄²⁻. While some methods require excessive energy requirements (e.g., 10³–10⁵ kWh/m³ for persulfate advanced oxidation),⁴⁶ recent studies have reported PFOA degradation at relatively high efficiency under ideal conditions using alkaline UV/sulfite advanced reduction (16 kWh/m³),⁴⁷ reactive electrochemical membranes (5.1 kWh/m³),⁴⁸ and plasma-based treatment (1.7 kWh/m³).⁴⁹ With a fully optimized reactor system, and incorporating future advances in the catalyst materials themselves, photocatalysis is deserving of further study as a PFAS treatment option alongside these other tools.

CONCLUSIONS

The data herein affirm that UV/BOHP effectively degrades long-chain PFCAs in acidified pure water through direct reaction with photogenerated h_{ν}^+ . Application to certain real waters may present cost-effectiveness challenges due to the potential for quenching by Cl⁻ and SO₄²⁻. Waters with high alkalinity may also be unsuitable for UV/BOHP, as acidifying such influents to the effective pH range with HCl resulted in similar inhibitory anion content. Our experiments showed that the inability of BOHP and other photocatalysts to degrade shorter-chain PFAS may be offset by incorporating VUV photolytic effects in the design of the reactor system. Future development of catalysts with highly positive surface charge is also recommended for targeting a wider range of PFAS compounds. Finally, we conclude that the focus on degradation kinetics as the primary performance metric for photocatalytic water treatment methods can obscure important differences in the energy efficiencies offered by different reactor designs. Reactors that treat larger volumes (relative to lamp power) at slower rates more effectively leverage photocatalytic effects and can achieve significantly lower EE/O values.

ASSOCIATED CONTENT

Supporting Information

The Supporting Information is available free of charge at <https://pubs.acs.org/doi/10.1021/acsestengg.0c00086>.

Experimental details of stock chemicals, instrumental analyses; photographs of reactors (Figure S1); PZC measurement of BOHP microparticles (Figure S2); tap water parameters (Table S1); geometric and operation time for bench-scale CHISPR with different annular widths (Table S2); NOM/UVT data (Figure S3); and LC-MS/MS PFCA detection limits (Table S3) (PDF)

AUTHOR INFORMATION

Corresponding Author

Ezra L. Cates – Department of Environmental Engineering and Earth Sciences, Clemson University, Anderson, South Carolina 29625, United States; orcid.org/0000-0003-0793-0246; Email: ecates@clemson.edu

Authors

Mojtaba Qanbarzadeh – Department of Environmental Engineering and Earth Sciences, Clemson University, Anderson, South Carolina 29625, United States

Dawei Wang – Department of Environmental Engineering and Earth Sciences, Clemson University, Anderson, South Carolina 29625, United States; orcid.org/0000-0002-3341-3544

Mohamed Ateia – Department of Chemistry, Northwestern University, Evanston, Illinois 60208, United States; orcid.org/0000-0002-3524-5513

Sushant P. Sahu – Department of Mechanical and Industrial Engineering, Louisiana State University, Baton Rouge, Louisiana 70803, United States

Complete contact information is available at:

<https://pubs.acs.org/10.1021/acsestengg.0c00086>

Author Contributions

[#]M.Q. and D.W. contributed equally to this work

Funding

This work was funded by the Strategic Environmental Research and Development Program (ER18-1599) and the Environmental Protection Agency STAR Early Career Award (RD83963).

Notes

The authors declare no competing financial interest.

ACKNOWLEDGMENTS

The authors wish to thank Tony Powell of Purifics Water Inc. for his discussions and advice.

REFERENCES

- (1) D'Agostino, L. A.; Mabury, S. A. Certain perfluoroalkyl and polyfluoroalkyl substances associated with aqueous film forming foam are widespread in Canadian surface waters. *Environ. Sci. Technol.* **2017**, *51*, 13603–13613.
- (2) Sun, M.; Arevalo, E.; Strynar, M.; Lindstrom, A.; Richardson, M.; Kearns, B.; Pickett, A.; Smith, C.; Knappe, D. R. U. Legacy and emerging perfluoroalkyl substances are important drinking water contaminants in the Cape Fear River watershed of North Carolina. *Environ. Sci. Technol. Lett.* **2016**, *3* (12), 415–419.
- (3) Wang, Z.; DeWitt, J. C.; Higgins, C. P.; Cousins, I. T. A never-ending story of per- and polyfluoroalkyl substances (PFASs)? *Environ. Sci. Technol.* **2017**, *51* (5), 2508–2518.
- (4) Lang, J. R.; Allred, B. M.; Field, J. A.; Levis, J. W.; Barlaz, M. A. National estimate of per- and polyfluoroalkyl substance (PFAS) release to U.S. municipal landfill leachate. *Environ. Sci. Technol.* **2017**, *51* (4), 2197–2205.

- (5) Ateia, M.; Attia, M. F.; Maroli, A.; Tharayil, N.; Alexis, F.; Whitehead, D. C.; Karanfil, T. Rapid removal of poly- and perfluorinated alkyl substances by poly(ethylenimine)-functionalized cellulose microcrystals at environmentally relevant conditions. *Environ. Sci. Technol. Lett.* **2018**, *5* (12), 764–769.

- (6) Xiao, L.; Ling, Y.; Alsbaiie, A.; Li, C.; Helbling, D. E.; Dichtel, W. R. β -Cyclodextrin polymer network sequesters perfluorooctanoic acid at environmentally relevant concentrations. *J. Am. Chem. Soc.* **2017**, *139* (23), 7689–7692.

- (7) Vecitis, C. D.; Park, H.; Cheng, J.; Mader, B. T.; Hoffmann, M. R. Treatment technologies for aqueous perfluorooctanesulfonate (PFOS) and perfluorooctanoate (PFOA). *Front. Environ. Sci. Eng. China* **2009**, *3* (2), 129–151.

- (8) Shao, T.; Zhang, P.; Jin, L.; Li, Z. Photocatalytic decomposition of perfluorooctanoic acid in pure water and sewage water by nanostructured gallium oxide. *Appl. Catal., B* **2013**, *142–143*, 654–661.

- (9) Wu, Y.; Li, Y.; Fang, C.; Li, C. Highly efficient degradation of perfluorooctanoic acid over a MnOx-modified oxygen-vacancy-rich In₂O₃ photocatalyst. *ChemCatChem* **2019**, *11*, 2297–2303.

- (10) Xu, J.; Wu, M.; Yang, J.; Wang, Z.; Chen, M.; Teng, F. Efficient photocatalytic degradation of perfluorooctanoic acid by a wide band gap p-block metal oxyhydroxide InOOH. *Appl. Surf. Sci.* **2017**, *416*, 587–592.

- (11) Duan, L.; Wang, B.; Heck, K.; Guo, S.; Clark, C. A.; Arredondo, J.; Wang, M.; Senfle, T. P.; Westerhoff, P.; Wen, X.; Song, Y.; Wong, M. S. Efficient photocatalytic PFOA degradation over boron nitride. *Environ. Sci. Technol. Lett.* **2020**, *7*, 613.

- (12) Sahu, S. P.; Qanbarzadeh, M.; Ateia, M.; Torzadeh, H.; Maroli, A. S.; Cates, E. L. Rapid degradation and mineralization of perfluorooctanoic acid by a new Petitjeanite Bi₃O(OH)(PO₄)₂ microparticle ultraviolet photocatalyst. *Environ. Sci. Technol. Lett.* **2018**, *5* (8), 533–538.

- (13) Krüger, J.; Winkler, P.; Lüderitz, E.; Lück, M.; Wolf, H. U. Bismuth, bismuth alloys, and bismuth Compounds. In *Ullmann's Encyclopedia of Industrial Chemistry*; Wiley-VCH Verlag GmbH & Co. KGaA: 2000.

- (14) McCullagh, C.; Robertson, P. K. J.; Adams, M.; Pollard, P. M.; Mohammed, A. Development of a slurry continuous flow reactor for photocatalytic treatment of industrial waste water. *J. Photochem. Photobiol., A* **2010**, *211* (1), 42–46.

- (15) Pujara, K.; Kamble, S. P.; Pangarkar, V. G. Photocatalytic degradation of phenol-4-sulfonic acid using an artificial UV/TiO₂ System in a slurry bubble column reactor. *Ind. Eng. Chem. Res.* **2007**, *46* (12), 4257–4264.

- (16) Chong, M. N.; Jin, B.; Chow, C. W. K.; Saint, C. Recent developments in photocatalytic water treatment technology: A review. *Water Res.* **2010**, *44* (10), 2997–3027.

- (17) Benotti, M. J.; Stanford, B. D.; Wert, E. C.; Snyder, S. A. Evaluation of a photocatalytic reactor membrane pilot system for the removal of pharmaceuticals and endocrine disrupting compounds from water. *Water Res.* **2009**, *43* (6), 1513–1522.

- (18) Purifics Water Inc. www.purifics.com (accessed 6/29/2020).

- (19) Gerrity, D.; Ryu, H.; Crittenden, J.; Abbaszadegan, M. Photocatalytic inactivation of viruses using titanium dioxide nanoparticles and low-pressure UV light. *J. Environ. Sci. Health, Part A: Toxic/Hazard. Subst. Environ. Eng.* **2008**, *43* (11), 1261–1270.

- (20) Chen, J.; Zhang, P.-y.; Liu, J. Photodegradation of perfluorooctanoic acid by 185 nm vacuum ultraviolet light. *J. Environ. Sci.* **2007**, *19* (4), 387–390.

- (21) Wang, Y.; Zhang, P. Effects of pH on photochemical decomposition of perfluorooctanoic acid in different atmospheres by 185 nm vacuum ultraviolet. *J. Environ. Sci.* **2014**, *26* (11), 2207–2214.

- (22) Li, X.; Zhang, P.; Jin, L.; Shao, T.; Li, Z.; Cao, J. Efficient photocatalytic decomposition of perfluorooctanoic acid by indium oxide and its mechanism. *Environ. Sci. Technol.* **2012**, *46* (10), 5528–5534.

- (23) Schneider, J. T.; Firak, D. S.; Ribeiro, R. R.; Peralta-Zamora, P. G. Use of scavenger agents in heterogeneous photocatalysis: truths, half-truths, and misinterpretations. *Phys. Chem. Chem. Phys.* **2020**, *22*, 15723.
- (24) Rodríguez, E. M.; Márquez, G.; Tena, M.; Álvarez, P. M.; Beltrán, F. J. Determination of main species involved in the first steps of TiO₂ photocatalytic degradation of organics with the use of scavengers: The case of ofloxacin. *Appl. Catal., B* **2015**, *178*, 44–53.
- (25) Sun, Y.; Li, G.; Wang, W.; Gu, W.; Wong, P. K.; An, T. Photocatalytic defluorination of perfluorooctanoic acid by surface defective BiOCl: Fast microwave solvothermal synthesis and photocatalytic mechanisms. *J. Environ. Sci.* **2019**, *84*, 69–79.
- (26) Lin, H.; Niu, J.; Ding, S.; Zhang, L. Electrochemical degradation of perfluorooctanoic acid (PFOA) by Ti/SnO₂-Sb, Ti/SnO₂-Sb/PbO₂ and Ti/SnO₂-Sb/MnO₂ anodes. *Water Res.* **2012**, *46* (7), 2281–2289.
- (27) Urtiaga, A.; Fernández-González, C.; Gómez-Lavín, S.; Ortiz, I. Kinetics of the electrochemical mineralization of perfluorooctanoic acid on ultrananocrystalline boron doped conductive diamond electrodes. *Chemosphere* **2015**, *129*, 20–26.
- (28) Mitchell, S. M.; Ahmad, M.; Teel, A. L.; Watts, R. J. Degradation of perfluorooctanoic acid by reactive species generated through catalyzed H₂O₂ propagation reactions. *Environ. Sci. Technol. Lett.* **2014**, *1* (1), 117–121.
- (29) Gagliano, E.; Sgroi, M.; Falciglia, P. P.; Vagliasindi, F. G. A.; Roccaro, P. Removal of poly- and perfluoroalkyl substances (PFAS) from water by adsorption: Role of PFAS chain length, effect of organic matter and challenges in adsorbent regeneration. *Water Res.* **2020**, *171*, 115381.
- (30) Bao, Y.; Deng, S.; Jiang, X.; Qu, Y.; He, Y.; Liu, L.; Chai, Q.; Mumtaz, M.; Huang, J.; Cagnetta, G.; Yu, G. Degradation of PFOA substitute: GenX (HFPO-DA Ammonium Salt): Oxidation with UV/persulfate or reduction with UV/sulfite? *Environ. Sci. Technol.* **2018**, *52* (20), 11728–11734.
- (31) Wang, W.; Maimaiti, A.; Shi, H.; Wu, R.; Wang, R.; Li, Z.; Qi, D.; Yu, G.; Deng, S. Adsorption behavior and mechanism of emerging perfluoro-2-propoxypropanoic acid (GenX) on activated carbons and resins. *Chem. Eng. J.* **2019**, *364*, 132–138.
- (32) Glaser, H. T.; Edzwald, J. K. Coagulation and direct filtration of humic substances with polyethylenimine. *Environ. Sci. Technol.* **1979**, *13* (3), 299–305.
- (33) Calza, P.; Pelizzetti, E. Photocatalytic transformation of organic compounds in the presence of inorganic ions. *Pure Appl. Chem.* **2001**, *73*, 1839.
- (34) Piscopo, A.; Robert, D.; Weber, J. V. Influence of pH and chloride anion on the photocatalytic degradation of organic compounds: Part I. Effect on the benzamide and para-hydroxybenzoic acid in TiO₂ aqueous solution. *Appl. Catal., B* **2001**, *35* (2), 117–124.
- (35) Wang, K.-H.; Hsieh, Y.-H.; Wu, C.-H.; Chang, C.-Y. The pH and anion effects on the heterogeneous photocatalytic degradation of o-methylbenzoic acid in TiO₂ aqueous suspension. *Chemosphere* **2000**, *40* (4), 389–394.
- (36) Lair, A.; Ferronato, C.; Chovelon, J.-M.; Herrmann, J.-M. Naphthalene degradation in water by heterogeneous photocatalysis: An investigation of the influence of inorganic anions. *J. Photochem. Photobiol., A* **2008**, *193* (2), 193–203.
- (37) Farmer Budarz, J.; Turolla, A.; Piasecki, A. F.; Bottero, J.-Y.; Antonelli, M.; Wiesner, M. R. Influence of aqueous inorganic anions on the reactivity of nanoparticles in TiO₂ Photocatalysis. *Langmuir* **2017**, *33* (11), 2770–2779.
- (38) Wiszniewski, J.; Robert, D.; Surmacz-Gorska, J.; Miksch, K.; Weber, J.-V. Photocatalytic mineralization of humic acids with TiO₂: Effect of pH, sulfate and chloride anions. *Int. J. Photoenergy.* **2003**, *5* (2), 69.
- (39) Iguchi, S.; Teramura, K.; Hosokawa, S.; Tanaka, T. Effect of the chloride ion as a hole scavenger on the photocatalytic conversion of CO₂ in an aqueous solution over Ni-Al layered double hydroxides. *Phys. Chem. Chem. Phys.* **2015**, *17* (27), 17995–18003.
- (40) Abdullah, M.; Low, G. K. C.; Matthews, R. W. Effects of common inorganic anions on rates of photocatalytic oxidation of organic carbon over illuminated titanium dioxide. *J. Phys. Chem.* **1990**, *94* (17), 6820–6825.
- (41) Kishimoto, N.; Doda, K. Effects of pH and coexisting chemicals on photolysis of perfluorooctane sulfonate using an excited xenon dimer lamp. *Water Sci. Technol.* **2018**, *77* (1), 108–113.
- (42) Duca, C.; Imoberdorf, G.; Mohseni, M. Effects of inorganics on the degradation of micropollutants with vacuum UV (VUV) advanced oxidation. *J. Environ. Sci. Health, Part A: Toxic/Hazard. Subst. Environ. Eng.* **2017**, *52* (6), 524–532.
- (43) Furatian, L. Advanced oxidation radiation: Unlocking the hidden power of low-pressure mercury lamps. *UV Solutions*, 2019; pp 33–37.
- (44) Crittenden, J. C.; Trussell, R. R.; Hand, D. W.; Howe, K. J.; Tchobanoglous, G. *Water Treatment Principles and Design*; John Wiley & Sons: 2012.
- (45) Sauer, T.; Cesconeto Neto, G.; José, H. J.; Moreira, R. F. P. M. Kinetics of photocatalytic degradation of reactive dyes in a TiO₂ slurry reactor. *J. Photochem. Photobiol., A* **2002**, *149* (1), 147–154.
- (46) Yang, L.; He, L.; Xue, J.; Ma, Y.; Xie, Z.; Wu, L.; Huang, M.; Zhang, Z. Persulfate-based degradation of perfluorooctanoic acid (PFOA) and perfluorooctane sulfonate (PFOS) in aqueous solution: Review on influences, mechanisms and prospective. *J. Hazard. Mater.* **2020**, *393*, 122405.
- (47) Bentel, M. J.; Liu, Z.; Yu, Y.; Gao, J.; Men, Y.; Liu, J. Enhanced degradation of perfluorocarboxylic acids (PFCAs) by UV/sulfite treatment: Reaction mechanisms and system efficiencies at pH 12. *Environ. Sci. Technol. Lett.* **2020**, *7* (5), 351–357.
- (48) Le, T. X. H.; Haflich, H.; Shah, A. D.; Chaplin, B. P. Energy-efficient electrochemical oxidation of perfluoroalkyl substances using a Ti₄O₇ reactive electrochemical membrane anode. *Environ. Sci. Technol. Lett.* **2019**, *6* (8), 504–510.
- (49) Singh, R. K.; Multari, N.; Nau-Hix, C.; Anderson, R. H.; Richardson, S. D.; Holsen, T. M.; Mededovic Thagard, S. Rapid removal of poly- and perfluorinated compounds from investigation-derived waste (IDW) in a pilot-scale plasma reactor. *Environ. Sci. Technol.* **2019**, *53* (19), 11375–11382.